Immunohistochemical Analysis of Olfactory Sensory Neuron Populations in the Developing Olfactory Organ of the Guppy, Poecilia reticulata (Cyprinodontiformes, Poecilidae)

OXFORD UNIVERSITY PRESS | Microscopy and Microanalysis

Immunohistochemical analysis of olfactory sensory neuron populations in the developing olfactory organ of the guppy, Poecilia reticulata (Cyprinodontiformes, Poecilidae)

Journal:	*Microscopy and Microanalysis*
Manuscript ID	MAM-23-120.R1
Manuscript Type:	Original Article
Date Submitted by the Author:	n/a
Complete List of Authors:	Bettini, Simone; University of Bologna, Biological, Geological and Environmental Sciences Lazzari, Maurizio; University of Bologna, Department of Biological, Geological and Environmental Sciences Milani, Liliana; University of Bologna, Department of Biological, Geological and Environmental Sciences Maurizii, Maria; University of Bologna, Department of Biological, Geological and Environmental Sciences Franceschini, Valeria; University of Bologna, Department of Biological, Geological and Environmental Sciences
Keywords:	olfactory epithelium, olfactory sensory neurons, crypt cells, immunohistochemistry, guppy
Abstract:	Olfaction is fundamental for sensing environmental chemicals and has obvious adaptive advantages. In fish, the peripheral olfactory organ is composed of lamellae in which the olfactory mucosa contains three main categories of olfactory sensory neurons (OSNs): ciliated (cOSNs), microvillous (mOSNs), and crypt cells. We studied the appearance of these different OSNs during development of Poecilia reticulata, given its growing use as animal model system. We performed immunohistochemical detection of molecular markers specific for the different OSNs, carrying out image analyses for marked-cell counting and measuring optical density. P. reticulata olfactory organ did not show change in size during the first weeks of life. The proliferative activity increased at the onset of secondary sexual characters, remaining high until sexual maturity. Then it decreased in both sexes, but with a recovery in females, probably in relation to their almost double body growth, compared to males. The density of both cOSNs and mOSNs remained constant throughout development, probably due to conserved functions already active in the fry, independently of the sex. The density of calretinin-positive crypt cells decreased progressively until sexual maturity, whereas the increased density of calretinin-negative crypt cell fraction, prevailing in later developmental stages, indicated their probable involvement in reproductive activities.

Immunohistochemical analysis of olfactory sensory neuron populations in the developing olfactory organ of the guppy, *Poecilia reticulata* (Cyprinodontiformes, Poecilidae)

Simone Bettini[1]†, Maurizio Lazzari[1]*†, Liliana Milani[1], Maria Gabriella Maurizii[1], Valeria Franceschini[1]

[1] Department of Biological, Geological and Environmental Sciences, University of Bologna, Via Selmi 3, 40126 Bologna, Italy

Olfactory sensory neuron populations in the guppy

Conflicts of interest: The authors declare none

* Author for correspondence:
Maurizio Lazzari, Department of Biological, Geological and Environmental Sciences, University of Bologna, Bologna 40126, Italy
E-mail: maurizio.lazzari@unibo.it
Phone number: +39 051 2094145

† The first two authors contributed equally to this work.

Abstract

Olfaction is fundamental for sensing environmental chemicals and has obvious adaptive advantages. In fish, the peripheral olfactory organ is composed of lamellae in which the olfactory mucosa contains three main categories of olfactory sensory neurons (OSNs): ciliated (cOSNs), microvillous (mOSNs), and crypt cells. We studied the appearance of these different OSNs during development of *Poecilia reticulata*, given its growing use as animal model system. We performed immunohistochemical detection of molecular markers specific for the different OSNs, carrying out image analyses for marked-cell counting and measuring optical density. *P. reticulata* olfactory organ did not show change in size during the first weeks of life. The proliferative activity increased at the onset of secondary sexual characters, remaining high until sexual maturity. Then it decreased in both sexes, but with a recovery in females, probably in relation to their almost double body growth, compared to males. The density of both cOSNs and mOSNs remained constant throughout development, probably due to conserved functions already active in the fry, independently of the sex. The density of calretinin-positive crypt cells decreased progressively until sexual maturity, whereas the increased density of calretinin-negative crypt cell fraction, prevailing in later developmental stages, indicated their probable involvement in reproductive activities.

Keywords: olfactory epithelium, olfactory sensory neurons, crypt cells, calretinin; $G_{\alpha\ olf}$, PCNA, guppy, immunohistochemistry, image analysis

Introduction

Olfaction is a phylogenetically ancient sense that has a very important role in animal life, being fundamentally related to food research and reproductive behavior (Zeiske et al., 1992). Vertebrates develop an olfactory system that detects odorants and pheromones through their interaction with specialized cell surface receptors on olfactory sensory neurons (OSNs). Olfaction is a form of chemosensation and sensing environmental chemicals has obvious adaptive advantages, thus it is not surprising that a diversity of chemosensory systems has evolved in animals (Poncelet & Shimeld, 2020).

The main types of fish olfactory sensory neurons (OSNs), common to all other vertebrates, are bipolar neurons with dendritic processes that reach the surface of the olfactory epithelium, where they originate olfactory terminal knobs bearing apical differentiations: cilia in ciliated OSNs (cOSNs) and microvilli in microvillous OSNs (mOSNs) (Riddle & Oakley, 1991; Hansen & Zeiske, 1998; Farbman, 2000). Ciliated olfactory sensory neurons (cOSNs) and microvillous olfactory sensory neurons (mOSNs) also differ in location of their cell bodies and length of their dendrites (Morita & Finger, 1998; Hamdani & Døving, 2007). Ciliated OSNs and mOSNs have sensitivities to partially overlapping odorant categories, but project into distinct regions of the olfactory bulb, related to different functions (Hansen et al., 2003; Hamdani & Døving, 2007; Braubach et al., 2012; Bazaes et al., 2013). Other than OSNs, the olfactory epithelium contains other cell types, such as sustentacular cells and basal stem cells.

Fish, in addition to the previously described OSN, also possess a third ovoid-shaped OSN type, the crypt cell (actinopterygian fish, Hansen et al., 1997; Hansen & Finger, 2000; cartilaginous fish, Ferrando et al., 2006, 2007). Crypt cells are located in the upper third of the olfactory epithelium and their apical pole facing the nasal cavity carries both cilia and microvilli. Their axonal projection patterns in the glomerular layer of the olfactory bulb are uneven among

species: in *Ictalurus puncatus* and *Carassius Carassius* crypt neuron terminals are localized to the ventral region, suggesting a possible association with pheromone perception and reproductive behavior (Hansen et al. 2003; Weltzien et al., 2003; Hamdani & Døving, 2006). On the other hand, in *Danio rerio*, crypt cells seem to project to one (Ahuja et al., 2013) or two (Braubach et al., 2012; Gayoso et al., 2012) dorsomedial glomeruli supposed to be connected with the medial olfactory tract, that is assumed to convey pheromone detection as well as alarm response (Ahuja et al., 2013). It is also controversial which odorants crypt cells respond to (Hamdani & Døving, 2006; Schmachtenberg, 2006; Hamdani et al., 2008; Vielma et al., 2008), so their function remains unclear. Other two OSN subtypes have been described: kappe cells and pear-shaped neurons (Ahuja et al., 2014; Wakisaka et al., 2017), but they have not currently been described in fish other than zebrafish and it is not sure if they can actually be defined as separate OSN types.

The peripheral olfactory organ of fish has a great variability in size, shape and organization in olfactory lamellae (Yamamoto, 1982; Hansen & Zielinski, 2005). With regard to the structure of the peripheral olfactory organ, fish can be distinguished into macrosmatic and microsmatic species (Lazzari et al., 2013). *Poecilia reticulata*, for example, possesses a small olfactory cavity containing a single olfactory lamella, therefore it is considered a typical representative of microsmatic fish (Lazzari et al., 2007).

Fish OSNs are directly exposed to environmental water and any substances it contains, toxicants included. Alterations in olfaction can affect fish behavior and survival with possible ecological and socio-economic consequences. *P. reticulata* has become an important model organism for developmental, ecological and toxicological studies (Kinnberg & Toft., 2003; Bettini et al., 2006; Antunes et al., 2017; Souza Trigueiro et al., 2021; Milani et al., 2022), and the acquisition of new information on the development and organization of the olfactory epithelium in this fish will allow us to extend and strengthen its use as model (Bettini et al., 2012, 2016, 2017).

Previously in our laboratory, we analyzed in adult *P. reticulata* both the histological and ultrastructural organizations of the peripheral olfactory organ (Lazzari et al., 2007), and the distribution of some molecular markers in the olfactory epithelium (Bettini et al., 2009). Particular attention was paid to crypt cells whose antigenic response in adults distinguished two subpopulations, supporting the possibility that crypt cells are functionally less uniform as supposed (Bettini et al., 2017). Our studies on the development of OSN populations in *P. reticulata* have been so far limited to a subpopulation of crypt cells ~~crypt cell subpopulation~~ (Bettini et al., 2012). The aim of this work is to study the dynamics of the populations of cOSNs, mOSNs, and a subpopulation of previously unexamined crypt cells, from fish birth to adulthood.

Materials and Methods

Animal care and breeding

Adult (older than 6months) *P. reticulata* (Peters, 1859) of both sexes were purchased locally from Coral Aquarium, Bologna, Italy, acclimated in laboratory conditions using separate aquaria for each sex containing a 1:2 mixture of dechlorinated tap water and distilled water at 27 °C in a 12/12 h light/dark cycle, and fed twice daily with commercial flake food. After 10 days, females were allowed to mate with males, at a ratio of 3:1 to reduce stressful conditions. In the following weeks, aquaria were daily monitored for pregnant females, that were isolated in tanks at the same conditions of aquaria and let give birth. All procedures conformed to the guidelines of European Communities Council Directive (86/609/CEE), the current Italian legislation regarding the use and care of animals, and the guidelines issued by the US National Institutes of Health. The Ethic-Scientific Committee of the University of Bologna also approved this study (protocol no. 17/79/2014).

Fry collection and tissue sampling

Newborn individuals were isolated immediately after birth in 5 L tanks and sacrificed at established time points (7, 14, 21, 45 and 90 days safter hatching). We included in the experiment also adult guppies (about 6-month-old). Fish were previously anesthetized with 0.1% 3-aminobenzoic acid ethyl ester (MS-222, Sigma Chemical, St. Louis, MO, USA) and immersion fixed in a modified Bouin's solution (saturated aqueous solution of picric acid and formalin at a ratio of 3:1) for 24 h. Heads from adult guppies were analogously collected and processed, after removal of dorsal cranial vault to facilitate fixation. All samples were washed several times in 0.1 M sodium phosphate buffer, pH 7.4, and decalcified in 10% ethylenediaminetetraacetic acid (EDTA, Fluka, Buchs, SG, CH) in the same buffer for 1-7 days, depending on specimen age and mineralization. Specimens were finally embedded in Paraplast plus (Sherwood Medical, St. Louis, MO, USA; melting point 55–57°C), frontally sectioned (5

μm) with Leica 2145 microtome (Leica Microsystems, Milan, IT) and mounted on silanized slides, two sections/slide. Sections of gonads were stained with Hematoxylin and Eosin to determine sex of guppy fry and sexual development.

Immunohistochemistry

Serial sections were selected for immunohistochemistry. Following stereological methods, every 10th pair of sections a disector was sampled (Bettini et al., 2009, 2012). Slides from 10 fish (5 males and 5 females) for each time point were processed. Sections were deparaffinized, rehydrated and immersed in 1% H_2O_2 (Sigma Chemical, St Louis, MO, USA) for 20 min at RT to quench endogenous peroxidase. Then antigen retrieval was performed with microwave treatment at 750 W for 10 min in citrate buffer at pH 6.0. Non-specific binding was blocked with 10% normal goat serum (NGS; Vector Laboratories, Burlingame, CA, USA) and 1% bovine serum agglutinin (BSA; Sigma Chemical~~, St Louis, MO, USA~~), before incubation in primary antibodies overnight at 4 °C. Then sections were washed and further incubated in horseradish peroxidase (HRP)-conjugated goat anti-rabbit IgG (1:100; Vector Laboratories) for polyclonal primary antibodies and goat anti-mouse IgG (1:100; A4416; Sigma) for monoclonal primary antibody. Finally, the immunoreaction was visualized with 0.1% 3,3-diaminobenzidine substrate (DAB; Sigma Chemical). Sections from zebrafish olfactory organ were chosen for positive controls. Negative controls were obtained by replacing the primary antibody with 10% NGS.

Antibodies

Primary antibodies used were: 1) polyclonal rabbit anti-calretinin (AB5054 [developed against rat calretinin], Chemicon International, Temecula, CA, USA, 1:1000), a marker for mOSNs (Bettini et al., 2009) and a subpopulation of crypt cells (Bettini et al., 2017); 2) polyclonal rabbit anti-$G_{\alpha\ olf}$ (sc-383; Santa Cruz Biotechnology, Santa Cruz, CA, USA, 1:500), a marker for cOSNs (Gayoso et al., 2011; Braubach et al., 2012; Bettini et al., 2016; Lazzari et al., 2017,

2019); 3) monoclonal mouse anti-proliferating cell nuclear antigen (anti-PCNA; Clone PC10; P 8825; Sigma; 1:500) to detect dividing cells (Bettini et al., 2016; Lazzari et al., 2017). All antibodies were already validated in previous literature: anti-calretinin in guppy (Bettini et al., 2017); anti-$G_{\alpha\ olf}$, which recognizes a 42-45 kDa protein under similar experimental conditions, in zebrafish (Gayoso et al., 2011; Braubach et al., 2012), in catfish (Hansen et al., 2003), in lamprey (Frontini et al., 2003), and in goldfish (Hansen et al., 2004).

Image acquisition and statistical analysis

Micrographs were taken using a BEL BlackL 5000 digital camera (BEL Engineering, Monza, Italy) mounted on an Olympus BH-2 microscope (Olympus Italia, Segrate, Italy).

Figures were assembled with Adobe Photoshop (CS3; Adobe Systems, San Jose, CA, USA), without content alteration.

We used the image analysis software ImageJ (version 1.53t) with Cell Counter plug-in (v.2) to count calretinin-positive crypt cells and PCNA-positive mitotic cells, and calculate epithelial volume and cell density (see Bettini et al., 2012 for more details). Immunostaining patterns of anti-$G_{\alpha\ olf}$ (cOSNs) and anti-calretinin (mOSNs) did not permit cell discrimination and counting (Bettini et al., 2016; Lazzari et al., 2017, 2019, 2021). Therefore, we considered the optical density (OD), since the immunostaining intensity can be regarded as an indirect index of the number of immunopositive cells (Iqbal & Byrd-Jacobs, 2010). In the olfactory epithelium, ImageJ analysis provided average gray values of immunostained regions and background-unstained zones. The OD was then calculated as the logarithm of the ratio between gray values of background and stained Region Of Interest (we excluded the lamina propria and exclusively selected the area of the epithelium, from the apical margin to the basal membrane). Using Excel 2019 (Microsoft Corporation, Redmond, WA, USA), data are reported in the histograms as means ± s.e.m. and statistically compared using one-way ANOVA (with LSD (Fisher Least

181 Significant Difference) *post hoc* test) for age groups, and Student's *t*-test for differences
182 between sexes in each group.
183

Results

In the first 3 time points considered (from 7 to 21 days of age), guppies were in the fry stage; in the 4th time point, at 45 days after birth, they were in the juvenile stage, when gonads reached their final structure, spermatogenesis started and oogenesis proceeded, secondary sexual characteristics developed and sexual dimorphism began to manifest; in the 5th time point, at 90 days of life fish were in the young stage and they were sexually active, even if sexual maturation was not complete: in females the eggs were not fully matured, while the males, despite having begun to court the females, were not yet capable to produce sperm and fertilize eggs. In the next three months they reached adult stage with fully developed gametes in both sexes ~~(Fig. 1)~~. At this point, fish size growth stopped or slowed down significantly. For more details see Evans et al. (2002) and Koya et al. (2003).

The olfactory organ of *Poecilia reticulata* contains only one olfactory lamella (Fig. 1a) whose surface is covered by the sensory epithelium (Fig. 1b). PCNA immunohistochemistry allowed to evaluate the course of cell proliferation during the considered periods. PCNA-positive cells were usually located in the basal region of the olfactory lamella (Figs. 2a1, 2b1, 2d1, 2a2, 2b2, 2d2). At stages of 7 and 14 days, the immunohistochemical staining was very reduced with very few positive cells detected in the lamellae of both sexes without significant difference between them (Figs. 2a1, 2a2, 2e). From 21 days onwards, the dimensional increase of the olfactory organ was due to a massive and statistically significant cell proliferation compared to the previous stage, but without significant differences between the two sexes (Fig. 2e). At 45 days, mitosis was still intense, comparable to the previous stage (Fig. 2e); the proliferating cells were mainly localized in the posterior edge of the lamella (Figs. 2b1, 2c1, 2b2, 2c2). In males at stage 90, upon reaching the sexual maturity, the proliferation decreased and stabilized showing values comparable to those found in adults. Instead, in females the proliferation continued and appeared to increase again after the mitotic rate decreased at 90 days of age (Fig. 2e). In adults,

PCNA-positive cells were still numerous and also present in all the basal layer of female olfactory lamella (Fig. 2d1), while in males they were restricted to some clusters in the posterior region of the lamella (Fig. 2d2). At adult stage, the volume of the olfactory lamella was about twice larger in females compared to males, in line with the ratio of total body size between females and males~~the relative proportions of the whole body of the two sexes~~ (Fig. 2f).

Anti-$G_{\alpha\ olf}$ antibody labeled the superficial knobs of ciliated OSNs whose cell bodies were located in the basal third of the olfactory epithelium and showed faint immunopositivity (Fig. 3a). The optical density of the immunopositive reaction evolved without significant difference between the two sexes and the various stages considered except for 21 and 45 days, in which the difference between sexes is significant, with the optical density being higher in males at 21 days and in females at 45 days (Fig. 3b). At 21 days of life, the optical density of males increased by about 45% compared to the averages measured in previous stages. From 45 days to adulthood the optical density of males returned to the average level recorded in previous fry stages. The optical density of females reached its higher value at 45 days, thus later than in males, then it decreased. However, the statistical analysis did not reveal significant differences between the various stages, even if both F values for females and males were very close to F critical values: female $F_{(P<0.05,5,24)}$=2.465 and male $F_{(P<0.05,5,24)}$=2.610; F critical=2.621.

Anti-calretinin immunopositivity was found in mOSNs whose cell bodies were located in the superficial half of the olfactory epithelium (Fig. 3c). The optical density of the immunohistochemical reaction showed no significant difference neither between sexes at any considered stage (Fig. 3d), nor between stages, even if, similarly to what observed for $G_{\alpha\ olf}$ immunohistochemistry, both F values for females and males were very close to F critical values: Female $F_{(P<0.05,5,24)}$=2.610 and male $F_{(P<0.05,5,24)}$=2.246; F Critical=2.621. Also in this case, the densities apparently increased in 45-day-old guppies.

In addition to mOSNs, anti-calretinin immunohistochemistry also detected a subpopulation of crypt neurons. The intense staining and the shape permitted their easy identification and counting: crypt cells had a typical rounded or ellipsoidal cell body placed close to the free surface of the olfactory epithelium (Figs. 4a, 4b). In the case of crypt cells, the total number of calretinin-positive cells is also ~~directly~~ presented, as their dynamics are exactly opposite to the trend of cell density. When considering the total number of calretinin-positive crypt cells, the value remained low, without significant differences among stages at 7, 14, 21 and 45 days after birth (Fig. 4c). Only in 90 days old fish, crypt cells were significantly more numerous in males than in females. Starting from 45 days onwards, there was a statistically significant increase in the total number of crypt cells compared to previous stages. The total number reached the highest values in adult males and females (Fig. 4c). When the density of immunopositive crypt cells was considered (Fig. 4d), the trend of the values obtained in the various stages appeared reversed compared to the trend of the total number of positive crypt cells. In fact, despite the moderate increase of the total number of calretinin-positive crypt cells, their density decreased up to the minimum value in the adult stage. In females, the density at 7 days after birth was significantly higher than other stages. In the following weeks the values gradually decreased until they stabilized from 45 days onwards. In males, on the other hand, significant differences in the density values of crypt cells among different stages were not observed. Significant differences between the two sexes were present only at 7 days, when the value was higher in females.

Comparing the number of calretinin-positive crypt cells obtained in this work with the total number of crypt cells, which are S100-positive, taken from our previous work (Bettini et al., 2009, 2012), we have drawn up Table 1 which shows the percentage ratio between these two types of crypt cells according to age and sex. The subpopulation of calretinin-positive crypt cells remains predominant in both sexes up to 3 weeks, with percentages ranging between 70%

and 90% (Table 1); from 45 days onwards, the ratio gradually decreases to 15% in females and 30% in males.

Discussion

The immunohistochemical localization of the selected molecular markers allowed us to follow the dynamics of the different populations of OSNs during the development of the olfactory mucosa of *P. reticulata*. From hatching up to the adult stage, the three main types of OSNs showed different behaviors. In particular, cOSNs and mOSNs showed constant density without particular differences between the stages. Sex-related differences appeared only for cOSNs at 21 and 45 days. Calretinin-positive crypt cells have decreasing density with age. Differences between sexes appeared only at 7 days.

In a previous work (Bettini et al., 2012), we observed that the dimensional increase of the olfactory organ of *P. reticulata* did not follow a linear trend: in the first 3 weeks the lamella did not undergo variations, and only afterwards there was an evident growth, which, after 90 days, led to a clear volumetric difference between males and females. In the present study, the analysis of proliferative activity shows an increase in mitotic cell number in both sexes between 21 and 45 days of life. PCNA-positive cells observed in the early stages of development are exclusively located in the basal layer of the epithelium. Due to their small number, we assume that they predominantly support normal neuronal turnover. The increase in volume does not affect the thickness, but the extent of the lamellar surface: from 21 days onwards, the greatest density of proliferating cells is found in the edges of the olfactory organ, in particular the caudal one, causing a progressive elongation of the lamella. At 90 days of age, the cell division rate stabilizes in males, remaining similar at the male adult stage, on the contrary it further increases in females in the adult stage, as their body growth continues to almost double the size of males. Mousavi-Sabet et al. (2014) reported numerous morphometric changes during the first 50 days of guppy development. While the growth in length of the body was quite progressive, allometric growth pattern of snout length became strongly positive between 15 and 20 days after birth, in line with what we observed in the olfactory organ. We can make some hypotheses in order to explain why the dimensional development of the olfactory organ undergoes this variation at

that particular stage. In fish, gonad formation begins 2 weeks before birth and their structure is established at 10-14 days post birth (Koya et al., 2003; Mazzoni et al., 2014). However, sex is unstable in the first weeks after birth and can be affected by administration of androgens, which can lead to sex reversal (Ortega-Salas et al., 2013). The formation of secondary sexual traits (caudal coloration, development of gonopodium in males, etc.), which starts approximately between 2 and 3 weeks of life, appears to be the first indication of guppy sexual identity (Houde, 1998; Evans et al., 2002; Koya et al., 2003). In fact, gametogenesis continues during the following weeks and is completed around 90-110 days after birth (Koya et al., 2003), but the formation of rod-shaped gonopodia with clearly visible apical hoods starts courtship activity in males, long before they can produce sperm (Houde, 1998; Evans et al., 2002). Since olfaction is involved in reproduction, the increase in size of the snout (and of the olfactory organ) could be correlated with the morpho-functional differentiation of the sex. But the absence of differences between male and female proliferation patterns could lead to another possible explanation. In accordance with Mousavi-Sabet et al. (2003), the rapid increase in *P. reticulata* snout elongation after 15 days may be related to changing feeding habit, i.e., foraging from water column to water surface.

Examining in more detail the development of the olfactory epithelium, we observed that the density of cONSs and mONSs remained constant from the first week of life up to the adult stage, with distinction between the two sexes only for cOSNs at 21 and 45 days. In the comparison between the stages, the apparent increase, however statistically not significant, which is visible for cOSNs between 21 and 45 days, could be a fluctuation simply reflecting the imbalance in the ratio among cell types caused by the intense proliferation activity. It appears evident that cOSNs and mOSNs are associated with the uptake of odorants linked to activities that are functionally independent of sex and stage of development. It is well known that foraging, social interaction, predator and toxicant avoidance and migration are the main

behaviors associated with smell in fish (Nikonov & Caprio, 2001; Bazaes et al., 2013; Olivares & Schmachtenberg, 2019).

Odorants have been indicatively divided in few molecular classes with different biological functions: amino acids, bile salts, nucleotides, polyamines and pheromones (Nikonov & Caprio, 2001; Sato & Sorensen, 2018). Numerous electrophysiological, behavioral and immunohistochemical studies, integrated with analysis of the molecular machinery of OSNs and their projection patterns, made it possible to associate some of those classes of odorants with each of the cell subtypes and suggest their role in the behavioral response (Bazaes et al., 2013; Olivares & Schmachtenberg, 2019). Both cOSNs and mOSNs appear to respond to amino acids in several teleost species (Sato & Suzuki, 2001; Hansen et al., 2003; Schmachtenberg & Bacigalupo, 2004), but cORNs respond preferentially to bile salts, whereas mOSNs are stimulated much more by amino acids and also by nucleotides (Hansen et al., 2003; Sato et al., 2005; Koide et al., 2009; Bazaes et al., 2013; Olivares & Schmachtenberg, 2019). Bile salts, mainly released into the water through feces and urine, are potential social odorants, that could play a role in identification of conspecifics, alarm response and territorial demarcation (Nikonov & Caprio, 2001; Hamdani & Døving, 2007; Bazaes et al., 2013). Nucleotides, instead, serve as feeding cues (Nikonov & Caprio, 2001; Hansen et al., 2003; Wakisaka et al., 2017; Sato & Sorensen, 2018). Amino acids are also a well-known category of food odorants (Hansen et al., 2003; Hara, 2006; Nikonov & Caprio, 2007; Miklavc & Valentinčič, 2012; Sato & Sorensen, 2018), but they appear to be also involved in behaviors other than feeding, such as homing (Yamamoto & Ueda, 2009) and reproduction (Yambe et al., 2006). Taken together these data seem to show that cOSNs are more correlated with social recognition among conspecifics, while mOSNs are more involved in the search for food, even if Biechl et al. (2016) showed that food odors stimulated both OSN subtypes, while only a subpopulation of mOSNs but not cOSNs detected kin odor related signal in zebrafish. These perceptions appear equally

important at all stages of development and the constant density of both cell types (cOSNs and mOSNs) that we observed during guppy development seems to be in accordance. However, at the moment the meaning of the difference between sexes at 21 and 45 days for cOSNs remains unclear. This difference could depend on an oscillation, although not significant, of the density values due to the increased proliferation of basal cells that in males is a few days earlier compared to females.

Interestingly, it has been observed that in the fish *Astyanax mexicanus*, present in two forms adapted to different environments, the proportions between cOSNs and mOSNs are different (Blin et al., 2018). COSNs were more represented in the surface-dwelling form, which is more oriented towards the sense of sight, while mOSNs were more abundant in the cave-adapted form, in which the sense of smell has predominant importance, given the reduction/absence of eyes. In both morphs, the proliferation, cell death, lifespan and neurogenesis patterns in the developing olfactory epithelium were identical, and very similar also between the two neuron subtypes, analogously to what we observed in guppies. It could have been interesting to compare the number of cOSNs and mOSNs in the guppy, but the immunohistochemical markers, especially the $G_{\alpha\ olf}$, do not allow easy cell counting, so we used an indirect estimate of densities, which thus cannot be compared. A possible solution to be considered to better distinguish and quantify the various OSN populations could be the use of transgenic fish, so far effectively tested by Ma et al. (2018) in zebrafish, but that will be hopefully possible in the future also for *P. reticulata*.

The third population of OSNs, crypt cells, has been associated to pheromone perception and reproduction in numerous studies (Hamdani & Døving, 2006; Bazáes & Schmachtenberg, 2012; Ahuja et al., 2013; Bazaes et al., 2013; Olivares & Schmachtenberg, 2019). As further support for this hypothesis, in *Carassius carassius* (Hamdani et al., 2008) the number of crypt cells varies throughout the year, increasing during the summer spawning season. Moreover, the

differentiation of crypt cells in the olfactory epithelium of the hermaphrodite *Pseudapocryptes lanceolatus* is synchronized with the annual development of ovarian structures in the summer, and they undergo apoptosis when the breeding season is over (Sarkar & De, 2018). We also observed that S100-positive crypt cell development correlates with sex and gonadal maturation in *P. reticulata*, with different dynamics and densities between males and females (Bettini et al., 2012). However, in another study (Bettini et al., 2017), we observed that crypt cells in *P. reticulata* do not constitute an immunohistochemically uniform population, identifying a subpopulation of calretinin-positive cells (the population analyzed in the present study). Also, Parisi et al. (2014) described, in zebrafish, a separate population of calretinin-positive crypt cells, even if they showed no co-localization of S100 and calretinin proteins. In the present study, we analyzed how this specific subpopulation of calretinin-positive crypt cells evolves during the first 6 months of postnatal life. Their number increases in line with epithelial size, with no substantial differences between males and females, even if in males it seems to start earlier. The density, however, remains almost constant in males and only slightly decreasing in females, with divergences between the two sexes at 7 days. Particularly interesting is the percentage ratio between this calretinin-positive subpopulation and the totality of crypt cells: at 7 days of life, calretinin-positive crypt cells are over 75% in both sexes, but this percentage gradually decreases after 3 weeks, reaching less than 30% in adult males and even 15% in adult females. It can be easily assumed that the two subpopulations have different functions: calretinin-positive cells, similarly to cOSNs and mOSNs, are linked to the perception of odors important from the first day of life to adulthood, while the other crypt cells become numerically preponderant only upon reaching sexual maturity, indicating a role connected to reproduction. Sandulescu et al. (2011) also described an early onset of crypt cell differentiation in zebrafish, at a stage similar to cOSNs and mOSNs, implying a probable functional significance in first life stages. It is known that crypt cells can respond to amino acids (Vielma et al., 2008);

moreover, in calcium imaging experiments on the rainbow trout (Bazáes & Schmachtenberg, 2012), it was observed that in young fish, crypt cells respond more to amino acids and bile salts, but in mature fish crypt cells are activated preferentially with exposure to gonadal extracts and hormones from the opposite sex. The authors suggested that, during development, the crypt cell population changed sensitivity and function, by replacing common odorant-sensitive cells with pheromone-sensitive ones. Complementing previous research (Bettini et al., 2012, 2017), present study appears to support the simultaneous presence of two distinct subpopulations of crypt neurons, with autonomous functions, modalities and times of development.

Conclusions

In this study we analyzed the development of the olfactory organ of *P. reticulata* that does not show a constant and progressive trend, but has a dimensional increase that begins three weeks after hatching with a massive proliferative activity. The density of cOSNs and mOSNs remains stable, with no differences between stages while sex related distinctions appear only for cOSNs at 21 and 45 days. Calretinin-positive crypt cell density decreases with age despite the simultaneous increase in the total number of these cells, probably due to a large increase in the size of the olfactory epithelium. The results suggest the role of cOSNs, mOSNs and calretinin-positive crypt cells in the uptake of odorants related to basic functions, such as search for food and social relations. However, many gaps remain in the understanding of the sensory capabilities of OSN subtypes, also because other factors influence the olfactory perception, making the data analysis very complex. Many factors appear to influence OSN sensitivity, as documented for example in zebrafish for the integration between alarm-response behavior and mating (Diaz-Verdugo et al., 2019), imprinting among siblings (Biechl et al., 2016), and neuropeptide expression (Kaniganti et al., 2021). Also, environmental changes can alter sensory capacity by modifying the composition of the epithelium, either for pollutants (Iqbal & Byrd-Jacobs, 2010; Dew et al., 2012, 2014, 2016; Lazzari et al., 2017, 2019, 2021) or by improving

412 the olfactory detection capacities, without affecting the organ size, as reported in visual-
413 deprived *Astyanax mexicanus* (Blin et al., 2018).

414 **Financial support**

415 This work was supported by national public funds grant RFO2021FRANCESCHINI from the
416 Italian Ministry of University and Research (MUR).

417

418 **Conflict of interest**

419 The authors declare that they have no conflicts of interest.

420
421

References

Ahuja G, Ivandić I, Saltürk M, Oka Y, Nadler W & Korsching SI (2013). Zebrafish crypt neurons project to a single, identified mediodorsal glomerulus. *Sci Rep* **3**, 2063. https://doi.org/10.1038/srep02063

Ahuja G, Nia SB, Zapilko V, Shiriagin V, Kowatschew D, Oka Y & Korsching SI (2014). Kappe neurons, a novel population of olfactory sensory neurons. *Sci Rep* **4**, 4037. https://doi.org/10.1038/srep04037

Antunes AM, Rocha TL, Pires FS, de Freitas MA, Milhomem Cruz Leite VR, Arana S, Moreira PC & Teixeira Saboia-Morais SM (2017). Gender-specific histopathological response in guppies *Poecilia reticulata* exposed to glyphosate or its metabolite aminomethylphosphonic acid. *J Appl Toxicol* **37**(9), 1098-1107. https://doi.org/10.1002/jat.3461

Bazáes A & Schmachtenberg O (2012). Odorant tuning of olfactory crypt cells from juvenile and adult rainbow trout. *J Exp Biol* **215**(10), 1740-1748. https://doi.org/10.1242/jeb.067264

Bazáes A, Olivares J & Schmachtenberg O (2013). Properties, projections, and tuning of teleost olfactory receptor neurons. *J Chem Ecol* **39**(4), 451-464. https://doi.org/10.1007/s10886-013-0268-1

Bettini S, Ciani F & Franceschini V (2006). Cell proliferation and growth-associated protein 43 expression in the olfactory epithelium in *Poecilia reticulata* after copper solution exposure. *Eur J Histochem* **50**(2), 141-146.

Bettini S, Lazzari M, Ciani F & Franceschini V (2009). Immunohistochemical and histochemical characteristics of the olfactory system of the guppy, *Poecilia reticulata* (Teleostei, Poecilidae). *Anat Rec (Hoboken)* **292**(10), 1569-1576. https://doi.org/10.1002/ar.20944

447 Bettini S, Lazzari M & Franceschini V (2012). Quantitative analysis of crypt cell population
448 during postnatal development of the olfactory organ of the guppy, *Poecilia reticulata*
449 (Teleostei, Poecilidae), from birth to sexual maturity. *J Exp Biol* **215**(15), 2711-2715.
450 https://doi.org/10.1242/jeb.069039
451 Bettini S, Lazzari M, Ferrando S, Gallus L & Franceschini V (2016). Histopathological analysis
452 of the olfactory epithelium of zebrafish (*Danio rerio*) exposed to sublethal doses of urea. *J*
453 *Anat* **228**(1), 59-69. https://doi.org/10.1111/joa.12397
454 Bettini S, Milani L, Lazzari M, Maurizii MG & Franceschini V (2017). Crypt cell markers in
455 the olfactory organ of *Poecilia reticulata*: analysis and comparison with the fish model
456 *Danio rerio*. *Brain Struct Funct* **222**(7), 3063-3074. https://doi.org/10.1007/s00429-017-
457 1386-2
458 Biechl D, Tietje K, Gerlach G & Wullimann MF (2016). Crypt cells are involved in kin
459 recognition in larval zebrafish. *Sci Rep* **6,** 24590. https://doi.org/10.1038/srep24590
460 Blin M, Tine E, Meister L, Elipot Y, Bibliowicz J, Espinasa L & Rétaux S (2018).
461 Developmental evolution and developmental plasticity of the olfactory epithelium and
462 olfactory skills in Mexican cavefish. *Dev Biol* **441**(2), 242-251.
463 https://doi.org/10.1016/j.ydbio.2018.04.019
464 Braubach OR, Fine A & Croll RP (2012). Distribution and Functional Organization of
465 Glomeruli in the Olfactory Bulbs of Zebrafish (*Danio rerio*). *J Comp Neurol* **520**(11),
466 2317-2339. https://doi.org/10.1002/cne.23075
467 Dew WA, Wood CM & Pyle GG (2012). Effects of continuous copper exposure and calcium
468 on the olfactory response of fathead minnows. *Environ Sci Technol* **46**(16), 9019-9026.
469 https://doi.org/10.1021/es300670p

Dew WA, Azizishirazi A & Pyle GG (2014). Contaminant-specific targeting of olfactory sensory neuron classes: connecting neuron class impairment with behavioural deficits. *Chemosphere* **112**, 519-525. https://doi.org/10.1016/j.chemosphere.2014.02.047

Dew WA, Veldhoen N, Carew AC, Helbing CC & Pyle GG (2016). Cadmium-induced olfactory dysfunction in rainbow trout: Effects of binary and quaternary metal mixtures. *Aquat Toxicol* **172**, 86-94. https://doi.org/10.1016/j.aquatox.2015.12.018

Diaz-Verdugo C, Sun GJ, Fawcett CH, Zhu P & Fishman MC (2019). Mating suppresses alarm response in zebrafish. *Curr Biol* **29**(15), 2541-2546.e3. https://doi.org/10.1016/j.cub.2019.06.047

Evans JP, Pitcher TE & Magurran AE (2002). The ontogeny of courtship, colour and sperm production in male guppies. *J Fish Biol* **60**(2), 495-498. https://doi.org/10.1111/j.1095-8649.2002.tb00299.x

Farbman AI (2000). Cell biology of olfactory epithelium. In The neurobiology of taste and smell, Finger TE, Silver WL & Restrepo D (Eds.), pp 131-158. New York: Wiley,

Ferrando S, Bottaro M, Gallus L, Girosi L, Vacchi M & Tagliafierro G (2006). Observations of crypt neuron-like cells in the olfactory epithelium of a cartilaginous fish. *Neurosci Lett* **403**(3), 280-282. https://doi.org/10.1016/j.neulet.2006.04.056

Ferrando S, Bottaro M, Pedemonte F, De Lorenzo S, Gallus L & Tagliafierro G (2007). Appearance of crypt neurons in the olfactory epithelium of the skate Raja clavata during development. *Anat Rec (Hoboken)* **290**(10), 1268-1272. https://doi.org/10.1002/ar.20584

Frontini A, Zaidi AU, Hua H, Wolak TP, Greer CA, Kafitz KW, Li W & Zielinski BS (2003). Glomerular territories in the olfactory bulb from the larval stage of the sea lamprey *Petromyzon marinus*. *J Comp Neurol* **465**(1), 27-37. https://doi.org/10.1002/cne.10811

493 Gayoso JÁ, Castro A, Anadón R & Manso MJ (2011). Differential bulbar and extra bulbar
494 projections of diverse olfactory receptor neuron populations in the adult zebrafish (*Danio*
495 *rerio*). *J Comp Neurol* **519**(2), 247-276. https://doi.org/10.1002/cne.22518
496 Gayoso J, Castro A, Anadón R & Manso MJ (2012). Crypt cells of the zebrafish Danio rerio
497 mainly project to the dorsomedial glomerular field of the olfactory bulb. *Chem Senses*
498 **37**(4), 357-369. https://doi.org/10.1093/chemse/bjr109
499 Hamdani EH & Døving KB (2006). Specific projection of the sensory crypt cells in the
500 olfactory system in crucian carp, *Carassius carassius*. *Chem Senses* **31**(1), 63-67.
501 https://doi.org/10.1093/chemse/bjj006
502 Hamdani EH & Døving KB (2007). The functional organization of the fish olfactory system.
503 *Prog Neurobiol* **82**(2), 80-86. https://doi.org/10.1016/j.pneurobio.2007.02.007
504 Hamdani EH, Lastein S, Gregersen F & Døving KB (2008). Seasonal variations in olfactory
505 sensory neurons—fish sensitivity to sex pheromones explained? *Chem Senses* **33**(2), 119-
506 123. https://doi.org/10.1093/chemse/bjm072
507 Hansen A & Finger TE (2000). Phyletic distribution of crypt-type olfactory receptor neurons
508 in fishes. *Brain Behav Evol* **55**(2), 100-110. https://doi.org/10.1159/000006645
509 Hansen A & Zeiske E (1998). The peripheral olfactory organ of the zebrafish, *Danio rerio*: an
510 ultrastructural study. *Chem Senses* **23**(1), 39-48. https://doi.org/39-48.
511 10.1093/chemse/23.1.39
512 Hansen A & Zielinski BS (2005). Diversity in the olfactory epithelium of bony fishes:
513 development, lamellar arrangement, sensory neuron cell types, and transduction
514 components. *J Neurocytol* **34**(3-5), 183-208. https://doi.org/10.1007/s11068-005-8353-1
515 Hansen A, Eller P, Finger TE & Zeiske E (1997). The crypt cell: a microvillous ciliated
516 olfactory receptor cell in teleost fishes. Nineteenth annual meeting of the association for
517 chemoreception sciences (AchemS XIX) and the twelfth international symposium on

518 olfaction and taste (ISOT XII) *Chem Senses* **22**(6), 694-695.
519 https://doi.org/10.1093/chemse/22.6.635
520 Hansen A, Rolen SH, Anderson K, Morita Y, Caprio J & Finger TE (2003). Correlation between
521 olfactory receptor cell type and function in the channel catfish. *J Neurosci* **23**(28), 9328 -
522 9339. https://doi.org/10.1523/JNEUROSCI.23-28-09328.2003
523 Hansen A, Anderson KT & Finger TE (2004). Differential distribution of olfactory receptor
524 neurons in goldfish: structural and molecular correlates. *J Comp Neurol* **477**(4), 347-359.
525 https://doi.org/10.1002/cne.20202
526 Hara TJ (2006). Feeding behaviour in some teleosts is triggered by single amino acids primarily
527 through olfaction. *J Fish Biol* **68**(3), 810-825. https://doi.org/10.1111/j.0022-
528 1112.2006.00967.x
529 Houde AE (1998). 2. Reproductive biology and sexual behavior. In *Sex, color, and mate choice*
530 *in guppies*, Houde AE (Ed.), pp. 29-44. Princeton: Princeton University Press.
531 https://doi.org/10.1515/9780691207261-003
532 Iqbal T & Byrd-Jacobs C (2010). Rapid degeneration and regeneration of the zebrafish
533 olfactory epithelium after triton X-100 application. *Chem Senses* **35**(5), 351-361.
534 https://doi.org/10.1093/chemse/bjq019
535 Kaniganti T, Deogade A, Maduskar A, Mukherjee A, Guru A, Subhedar N & Ghose A
536 (2021). Sensitivity of olfactory sensory neurons to food cues is tuned to nutritional states
537 by Neuropeptide Y signaling. *J Neurochem* **159**(6), 1028-1044.
538 https://doi.org/10.1111/jnc.15488
539 Kinnberg K & Toft G (2003). Effects of estrogenic and antiandrogenic compounds on the testis
540 structure of the adult guppy (*Poecilia reticulata*). *Ecotoxicol Environ Saf* **54**(1), 16-24.
541 https://doi.org/10.1016/s0147-6513(02)00010-6

Koide T, Miyasaka N, Morimoto K, Asakawa K, Urasaki A, Kawakami K & Yoshihara Y (2009). Olfactory neural circuitry for attraction to amino acids revealed by transposon mediated gene trap approach in zebrafish. *Proc Natl Acad Sci USA* **106**(24), 9884-9889. https://doi.org/10.1073/pnas.0900470106

Koya Y, Fujita A, Niki F, Ishihara E & Miyama H (2003). Sex differentiation and pubertal development of gonads in the viviparous mosquitofish, *Gambusia affinis*. *Zoolog Sci* **20**(10), 1231-1242. https://doi.org/10.2108/zsj.20.1231

Lazzari M, Bettini S, Ciani F & Franceschini V (2007). Light and transmission electron microscopy study of the peripheral olfactory organ of the guppy, *Poecilia reticulata* (Teleostei, Poecilidae). *Microsc Res Tech* **70**(9), 782-789. https://doi.org/10.1002/jemt.20487

Lazzari M, Bettini S & Franceschini V (2013). Immunocytochemical characterization of olfactory ensheathing cells in fish. *Brain Struct Funct* **218**(2), 539-549. https://doi.org/10.1007/s00429-012-0414-5

Lazzari M, Bettini S, Milani L, Maurizii MG & Franceschini V (2017). Differential response of olfactory sensory neuron populations to copper ion exposure in zebrafish. *Aquatic Toxicol* **183**, 54-62. https://doi.org/10.1016/j.aquatox.2016.12.012

Lazzari M, Bettini S, Milani L, Maurizii MG & Franceschini V (2019). Differential nickel-induced responses of olfactory sensory neuron populations in zebrafish. *Aquatic Toxicol* **206**, 14-23. https://doi.org/10.1016/j.aquatox.2018.10.011

Lazzari M, Bettini S, Milani L, Maurizii MG & Franceschini V (2021). Response of olfactory sensory neurons to mercury ions in zebrafish: an immunohistochemical study. *Microsc Microanal* **28**(1), 227-242. https://doi.org/10.1017/S1431927621013763

Ma EY, Heffern K, Cheresh J & Gallagher EP (2018). Differential copper-induced death and regeneration of olfactory sensory neuron populations and neurobehavioral function in

larval zebrafish. *Neurotoxicology* **69,** 141-151. https://doi.org/10.1016/j.neuro.2018.10.002

Mazzoni TS, Grier HJ & Quagio-Grassiotto I (2014). Male gonadal differentiation and the paedomorphic evolution of the testis in teleostei. *Anat Rec* **297**(6), 1137-1162. https://doi.org/10.1002/ar.22915

Miklavc P & Valentinćić T (2012). Chemotopy of amino acids on the olfactory bulb predicts olfactory discrimination capabilities of zebrafish *Danio rerio*. *Chem Senses* **37**(1), 65-75. https://doi.org/10.1093/chemse/bjr066

Milani L, Cinelli F, Iannello M, Lazzari M, Franceschini V & Maurizii MG (2022). Immunolocalization of Vasa, PIWI, and TDRKH proteins in male germ cells during spermatogenesis of the teleost fish *Poecilia reticulata*. *Acta Histochem* **124**(3), 151870. https://doi.org/10.1016/j.acthis.2022.151870

Morita Y & Finger TE (1998). Differential projections of ciliated and microvillous olfactory receptor cells in the catfish, *Ictalurus punctatus*. *J Comp Neurol* **398**(4), 539-550. https://doi.org/10.1002/(sici)1096-9861(19980907)398:4<539::aid-cne6>3.0.co;2-3

Mousavi-Sabet H, Azimi H, Eagderi S, Bozorgi S & Mahallatipour B (2014). Growth and morphological development of guppy *Poecilia reticulata* (Cyprinodontiformes, Poeciliidae) larvae. *Poec Res* **4**(1), 24-30. http://www.pr.bioflux.com.ro/docs/2014.24-30.pdf

Nikonov AA & Caprio J (2001). Electrophysiological evidence for a chemotopy of biologically relevant odors in the olfactory bulb of the channel catfish. *J Neurophysiol* **86**(4), 1869-1876. https://doi.org/10.1152/jn.2001.86.4.1869

Nikonov AA & Caprio J (2007). Highly specific olfactory receptor neurons for types of amino acids in the channel catfish. *J Neurophysiol* **98**(4), 1909-1918. https://doi.org/10.1152/jn.00548.2007

592 Olivares J & Schmachtenberg O (2019). An update on anatomy and function of the teleost
593 olfactory system. *PeerJ* **7**, e7808. https://doi.org/10.7717/peerj.7808
594 Ortega-Salas A, Reyes-Bustamante H & Reyes BH (2013). Sex reversal, growth, and survival
595 in the guppy *Poecilia reticulata* (Cyprinodontiformes: Poeciliidae) under laboratory
596 conditions. *UNED Res J* **5**(2), 245-248. https://doi.org/10.22458/urj.v5i2.278
597 Parisi V, Guerrera MC, Abbate F, Garcia-Suarez O, Viña E, Vega JA & Germanà A (2014).
598 Immunohistochemical characterization of the crypt neurons in the olfactory epithelium of
599 adult zebrafish. *Ann Anat* **196**, 178-182. https://doi.org/10.1016/j.aanat.2014.01.004
600 Poncelet G & Shimeld SM (2020). The evolutionary origins of the vertebrate olfactory system.
601 *Open Biol* **10**(12), 200330. https://doi.org/10.1098/rsob.200330
602 Riddle DR & Oakley B (1991). Evaluation of projection patterns in the primary olfactory
603 system of rainbow trout. *J Neurosci* **11**(12), 3752-3762.
604 https://doi.org/10.1523/JNEUROSCI.11-12-03752.1991
605 Sandulescu CM, Teow RY, Hale ME & Zhang C (2011). Onset and dynamic expression of
606 S100 proteins in the olfactory organ and the lateral line system in zebrafish development.
607 *Brain Res* **1383**, 120-127. https://doi.org/10.1016/j.brainres.2011.01.087
608 Sarkar SK & De SK (2018). Ultrastructure based morphofunctional variation of olfactory crypt
609 neuron in a monomorphic protogynous hermaphrodite mudskipper (Gobiidae:
610 Oxudercinae) (*Pseudapocryptes lanceolatus* [Bloch and Schneider]). *J Microsc Ultrastruct*
611 **6**(2), 99-104. https://doi.org/10.4103/JMAU.JMAU_18_18
612 Sato K & Sorensen PW (2018). The chemical sensitivity and electrical activity of individual
613 olfactory sensory neurons to a range of sex pheromones and food odors in the goldfish.
614 *Chem Senses* **43**(4), 249-260. https://doi.org/10.1093/chemse/bjy016

615 Sato K & Suzuki N (2001). Whole-cell response characteristics of ciliated and microvillous
616 olfactory receptor neurons to amino acids, pheromone candidates and urine in rainbow
617 trout. *Chem Senses* **26**(9), 1145-1156. https://doi.org/10.1093/chemse/26.9.1145

618 Sato Y, Miyasaka N & Yoshihara Y (2005). Mutually exclusive glomerular innervation by two
619 distinct transgenic zebrafish. *J Neurosci* **25**(20), 4889-4897.
620 https://doi.org/10.1523/JNEUROSCI.0679-05.2005

621 Schmachtenberg O (2006). Histological and electrophysiological properties of crypt cells from
622 the olfactory epithelium of the marine teleost *Trachurus symmetricus*. *J Comp Neurol*
623 **495**(1), 113-121. https://doi.org/10.1002/cne.20847

624 Schmachtenberg O & Bacigalupo J (2004). Olfactory transduction in ciliated receptor neurons
625 of the Cabinza grunt, *Isacia conceptionis* (Teleostei: Haemulidae). *Eur J Neurosci* **20**(12),
626 3378-3386. https://doi.org/10.1111/j.1460-9568.2004.03825.x

627 Souza Trigueiro NS, Gonçalves BB, Cirqueira Diaz F, Celmade Oliveira Lima E, Lopes Rocha
628 T & Teixeira Saboia-Morais SM (2021). Co-exposure of iron oxide nanoparticles and
629 glyphosate-based herbicide induces DNA damage and mutagenic effects in the guppy
630 (*Poecilia reticulata*). *Environ Toxicol Pharmacol* **81**, 103521.
631 https://doi.org/10.1016/j.etap.2020.103521

632 Vielma A, Ardiles A, Delgado L & Schmachtenberg O (2008). The elusive crypt olfactory
633 receptor neuron: evidence for its stimulation by amino acids and cAMP pathway agonists.
634 *J Exp Neurol* **211**(15), 2417-2422. https://doi.org/10.1242/jeb.018796

635 Wakisaka N, Miyasaka N, Koide T, Masuda M, Hiraki-Kajiyama T & Yoshihara Y (2017). An
636 adenosine receptor for olfaction in fish. *Curr Biol* **27**(10), 1437-1447.
637 https://doi.org/10.1016/j.cub.2017.04.014

638 Weltzien FA, Hoglund E, Hamdaniel H & Døving KB (2003). Does the lateral bundle of the
639 medial olfactory tract mediate reproductive behavior in male crucian carp? *Chem Senses*
640 **28**(4), 293-300. https://doi.org/10.1093/chemse/28.4.293
641 Yamamoto M (1982). Comparative morphology of the peripheral olfactory organ in teleosts. In
642 *Chemoreception in fishes*, Hara TJ (Ed.), pp. 39–59. Amsterdam: Elsevier.
643 Yamamoto Y & Ueda H (2009). Behavioral responses by migratory chum salmon to amino
644 acids in natal stream water. *Zoolog Sci* **26**(11), 778-782. https://doi.org/10.2108/zsj.26.778
645 Yambe H, Kitamura S, Kamio M, Yamada M, Matsunaga S, Fusetani N & Yamazaki F (2006).
646 L-Kynurenine, an amino acid identified as a sex pheromone in the urine of ovulated female
647 masu salmon. *Proc Natl Acad Sci USA* **103**(42), 15370-15374.
648 https://doi.org/10.1073/pnas.0604340103
649 Zeiske E, Theisen B & Breucker H (1992). Structure, development and evolutionary aspects of
650 the peripheral olfactory system. In *Fish Chemoreception*, Hara TJ (Ed.), pp. 13-39.
651 London: Chapman and Hall.
652

Figure legends

Fig. 1. Light microscopic organization of the olfactory organ of adult *Poecilia reticulata*. (**a**) In a frontal section of the head, the left olfactory organ appears composed of a single lamella (arrowheads) protruding into the olfactory cavity. (**b**) Histological organization of the olfactory epithelium (E) covering the olfactory lamella. LP, lamina propria. Hematoxylin-eosin. Scale bars (a), 200 µm; (b), 20 µm. ~~Gonads of 6-month-old *Poecilia reticulata* (Haematoxylin and Eosin). (**a**) Oocyte, characterized by abundant yolk and large lipid globules, in the adult ovary. (**b**) Spermatozoa located in groups of spermatozeugmata in the mature cysts of adult testis. Scale bar (1a, 1b), 100 µm.~~

Fig. 2. PCNA immunohistochemistry. (**a1, a2**) Representative micrographs of lamellae with mitotic cells in the basal layer (arrowheads) in 7-day-old female (a1) and male (a2) guppies. (**b1, b2**) Representative micrographs of lamellae in 45-day-old female (b1) and male (b2) guppies: dividing cells are more concentrated in the ~~caudal~~ posterior region of the olfactory organ (arrows) than in the basal layer of the central and rostral lamella (arrowhead). (**c1, c2**) Higher magnification of the caudal region of the olfactory lamella in 45-day-old female (c1) and male (c2). (**d1, d2**) Representative micrographs of the lamellae in adult female (d1) and male (d2) guppies: the PCNA-positive cells are mainly located in the ~~caudal~~ posterior edge of male olfactory organ (arrow), while in females they are also visible along the basal layer of the entire lamella (arrowheads). C, caudal; R, rostral; L, lateral; M, medial. Scale bars (a1-b2, d1, d2), 100 µm; (c1, c2), 10 µm. (**e**) Density of proliferating cells and statistical comparison among life stages and between sexes. (**f**) Volume of the olfactory lamella in adult females and males. Significant differences among stages are indicated by asterisks above the bars, while differences between sexes for each sampling time are indicated by asterisks superimposed on the bars.

677 Continuous lines, female/female comparison; dotted lines, male/male comparison. *P<0.05,
678 **P<0.01, N=10.
679
680 **Fig. 3.** $G_{\alpha\ olf}$ and calretinin immunohistochemistry. (**a**) Representative micrograph of lamellae
681 with $G_{\alpha\ olf}$-positive cells: immunostaining is mostly visible in the apical knobs of cOSNs
682 (arrows) but is also present in the cytoplasm of cells throughout the lower half of the epithelium
683 (arrowheads). Scale bar (a), 20 µm. (**b**) Optical density values of $G_{\alpha\ olf}$-positive cOSNs and
684 statistical comparison among life stages and between sexes. Asterisks indicate significant
685 male/female differences. *P<0.05, N=10. (**c**) Representative micrograph of lamellae with
686 calretinin-positive cells: they are mOSNs localized in the upper half of the epithelium. Scale
687 bar (c), 20 µm. (**d**) Optical density values of calretinin-positive mOSNs; there are no significant
688 differences among stages and between sexes.
689
690 **Fig. 4.** Calretinin-positive crypt cells. (**a, b**) Representative micrographs of stained crypt
691 neurons with the characteristic ovoid shape (arrows); in some cases, the emerging axon is
692 clearly visible (arrowhead). Scale bar (a, b): 20 µm. (**c**) Histogram comparing the number of
693 calretinin-positive crypt cells per animal at various life stages. (**d**) Histogram comparing the
694 density of calretinin-positive crypt cells at various life stages. Significant differences among
695 stages are indicated by asterisks above the bars, while differences between sexes for each
696 sampling time are indicated by asterisks superimposed on the bars. Continuous lines,
697 female/female comparison; dotted lines, male/male comparison. *P<0.05, **P<0.01, N=10.
698

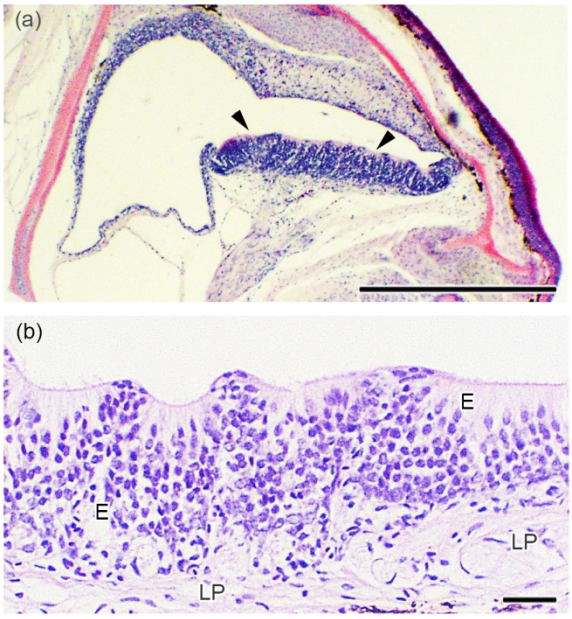

Fig. 1. Light microscopic organization of the olfactory organ of Poecilia reticulata

161x108mm (300 x 300 DPI)

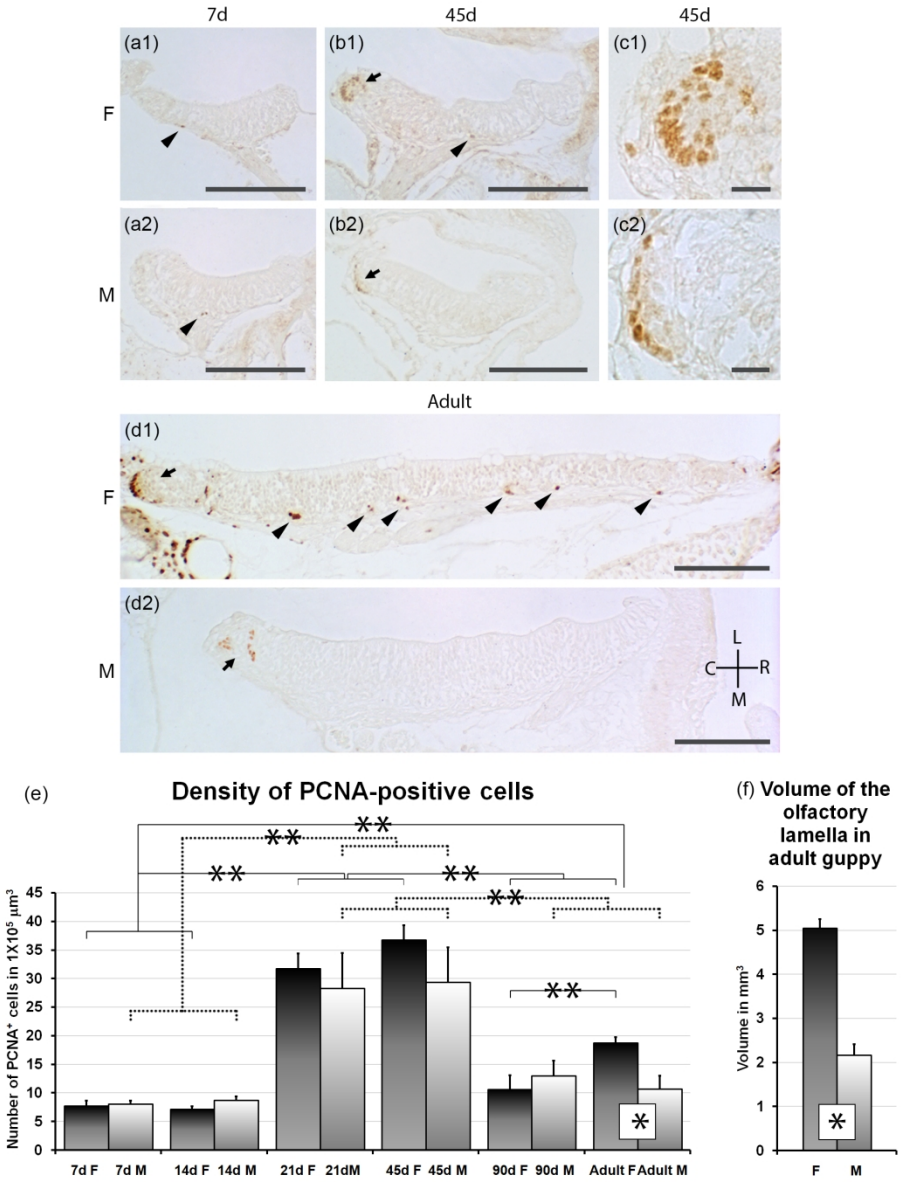

Fig. 2. PCNA immunohistochemistry

162x216mm (300 x 300 DPI)

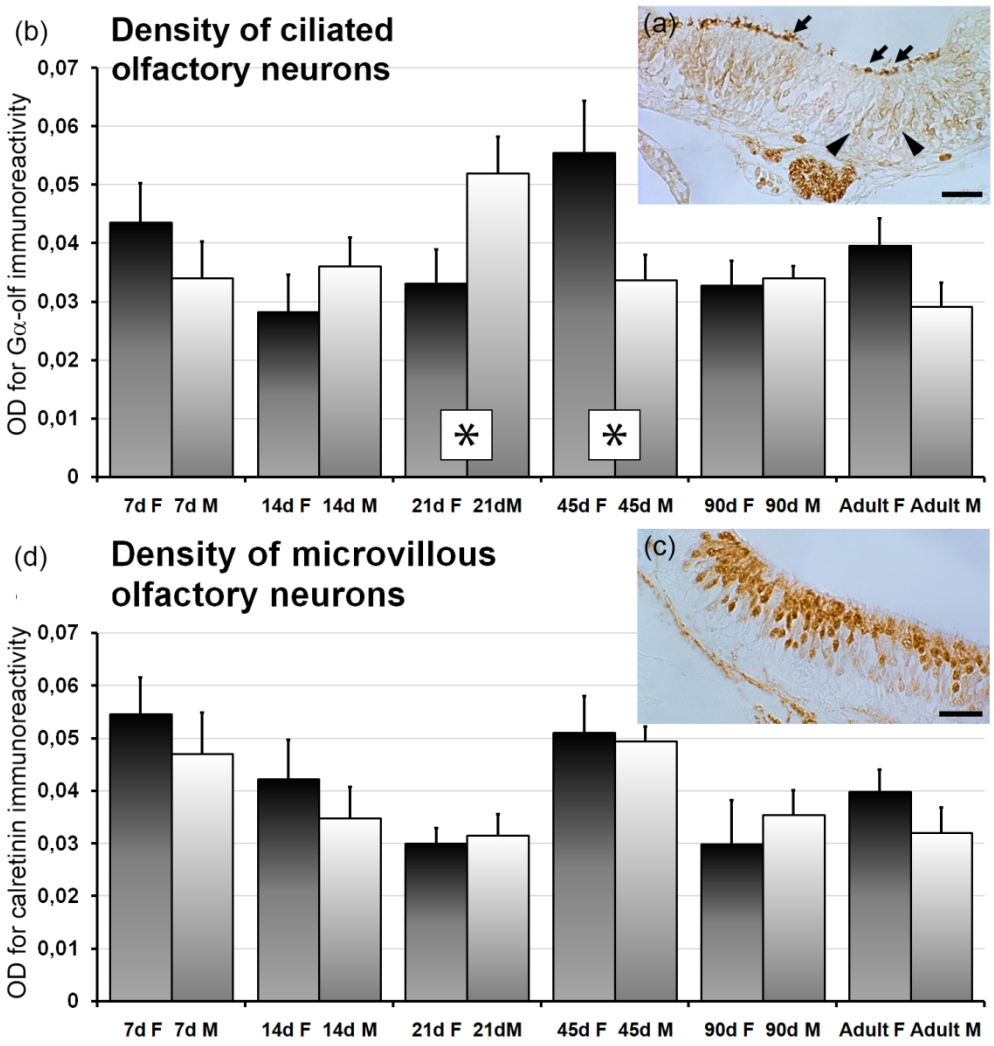

Fig. 3. $G_{\alpha\ olf}$ and calretinin immunohistochemistry.

127x133mm (300 x 300 DPI)

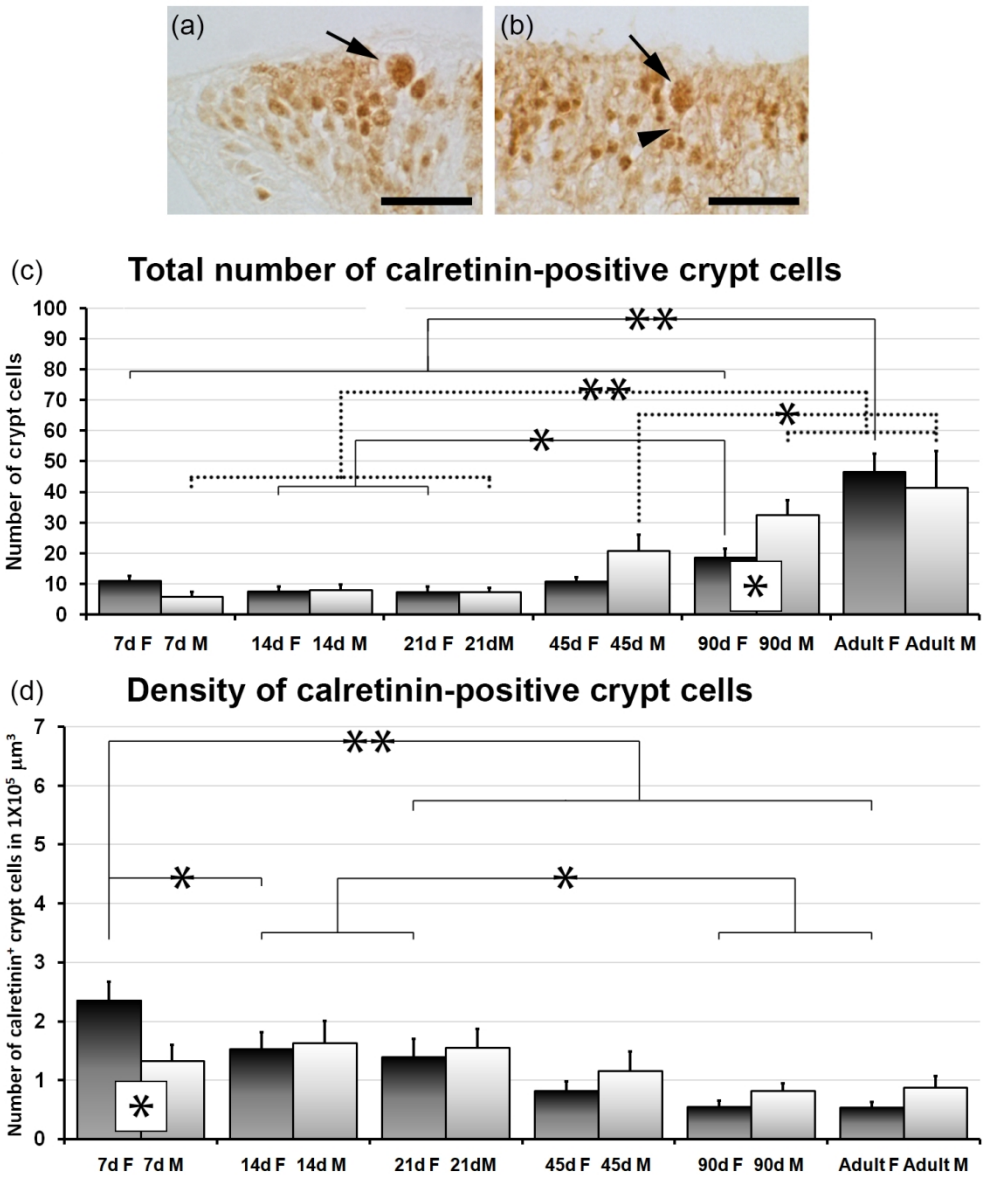

Fig. 4. Calretinin-positive crypt cells.

127x151mm (300 x 300 DPI)

Table 1. Number of calretinin-positive crypt cells, total number of crypt cells (S100-positive)*, and their percentage ratio according to age and sex.

FEMALE	Calretinin$^+$ crypt cells	Total number of crypt cells (S100$^+$)	$\frac{\text{Calretinin}^+ \text{ crypt cells}}{\text{S100}^+ \text{ crypt cells}}$ %
7d	10.8±1.3	13.8±1.4	77.93%
14d	7.7±1.3	9.2±1.7	84.28%
21d	7.4±1.8	8.4±1.3	88.02%
45d	10.9±1.3	27±3	40.62%
90d	19±3	77±6	24.36%
Adult	47±6	297±30	15.74%

MALE	Calretinin$^+$ crypt cells	Total number of crypt cells (S100$^+$)	$\frac{\text{Calretinin}^+ \text{ crypt cells}}{\text{S100}^+ \text{ crypt cells}}$ %
7d	5.97±1.5	8.5±1.5	70.65%
14d	7.98±1.8	8.7±0.8	91.4%
21d	7.48±1.3	9.9±0.9	75.4%
45d	21±5	28±2	74.81%
90d	33±5	61±5	53.81%
Adult	42±12	139±12	29.82%

Values are mean per animal ± s.e.m.

* Values taken from Bettini et al., 2009, 2012